Available online at www.sciencedirect.com
ScienceDirect
ELSEVIER
Palaeogeography, Palaeoclimatology, Palaeoecology 241 (2006) 440–456
PALAEO
www.elsevier.com/locate/palaeo

Holocene vegetation variations and the associated environmental changes in the western part of the Chinese Loess Plateau

Z.-D. Feng [a,b,*], L.Y. Tang [c], H.B. Wang [d], Y.Z. Ma [a], K.-b. Liu [e]

[a] *MOE Key Laboratory of Western China's Environmental Systems and College of Resource and Environmental Sciences, Lanzhou University, Lanzhou 73000, China*
[b] *Department of Earth and Environmental Studies, Montclair State University, Upper Montclair, NJ 07043, USA*
[c] *Nanjing Institute of Geology and Paleontology, CAS, Nanjing 210008, China*
[d] *College of Resource Science and Technology, Beijing Normal University, Beijing 100875, China*
[e] *Department of Geography and Anthropology, Louisiana State University, Baton Rouge, LA 70803, USA*

Received 4 May 2005; received in revised form 20 April 2006; accepted 27 April 2006

Abstract

The western part of the Chinese Loess Plateau has experienced a series of environmental changes during the Holocene. A desert-steppe of late glacial was succeeded by a forest-steppe from 8850 to 7540 ^{14}C years BP, and a *Pinus*-dominated forest occupied the landscape from 7540 to 6560 ^{14}C years BP. A deciduous forest of high density and diversity existed from 6560 to 5790 ^{14}C years BP. Afterwards the vegetation changed to a *Pinus*-dominated forest-steppe (5790–4950 ^{14}C years BP) and then to an *Ulmus*-dominated forest-steppe (4950 to ~4000 ^{14}C years BP). The vegetation subsequently changed to a steppe from ~4000 to 3120 ^{14}C years BP and further to a desert-steppe from 3120 to 2900 ^{14}C years BP. After a period of vegetation improvement (steppe) from 2900 to 2460 ^{14}C years BP, a desert-steppe resumed (2460–2020 ^{14}C years BP). Steppe vegetation was re-established around 2020 ^{14}C years BP and seems to have then deteriorated again around 1000 ^{14}C years BP. The general trend of aforementioned climatic changes is proposed here to have been modulated by the insolation changes. Specifically, the insolation started to increase around 15,000 years BP and peaked around 9000 years BP when the obliquity-driven seasonality reached a maximum with the summer insolation being about 8% more than the present. As a result, tropical Holocene SST increased steadily from ~10,000 to ~6,000 years BP, thus effectively strengthening the East Asian summer monsoon. In addition, the documented high temperatures from 10,000 to 4000 years BP in high northern latitudes might have weakened the strength of the winter monsoon and thus enhanced the strength of the summer monsoon probably via lengthening of the rainy season, directly contributing to the "megahumid" climate between 10,000 and 4000 years BP in the western part of the Chinese Loess Plateau.

Keywords: Holocene climate; Chinese Loess Plateau; Vegetation history

1. Introduction

1.1. Significance of Holocene climate changes

Possible human-induced climate changes and adverse human impacts on environment alert us to assess

* Corresponding author. Department of Earth and Environmental Studies, Montclair State University, Upper Montclair, NJ 07043, USA.
E-mail address: fengz@mail.montclair.edu (Z.-D. Feng).

0031-0182/$ - see front matter © 2006 Elsevier B.V. All rights reserved.
doi:10.1016/j.palaeo.2006.04.009

future climatic stability and environmental sustainability. However, this assessment requires a solid understanding of the natural climatic variability on different time scales. The Holocene (i.e., past 10,000 years) is of particular interest in that regard because the climatic boundary conditions are similar to those experienced now and possibly in the near future. To understand the global Holocene climate changes and the controlling mechanisms, the temporal and spatial climatic records are needed from different and climatically sensitive regions. The semiarid Chinese Loess Plateau has been demonstrated to be one of the most sensitive areas to large-scale climate changes (Feng et al., 1993; Li et al., 1988; Feng et al., 2004). Specifically, loess deposition itself on the plateau is a result of interactions between the winter and summer monsoons. That is, the winter monsoon brings dust onto the plateau and the summer monsoon-associated vegetation retains the dust (loess). Therefore, the reconstruction of the Holocene climate changes in the Chinese Loess Plateau is expected to significantly improve our understanding of the mechanisms and processes of large-scale climate changes. This study focuses on Holocene sequences in the western part of the plateau where higher-resolution reconstruction can be achieved simply because the sequences are much thicker (up to 5 m) than in the eastern part of the plateau. The Liupan Mountain is the dividing line between the western and eastern parts (Fig. 1). We hope that this regional climatic reconstruction can be useful in depicting the large-scale patterns of Holocene climate changes and thus in facilitating our understanding of the mechanisms.

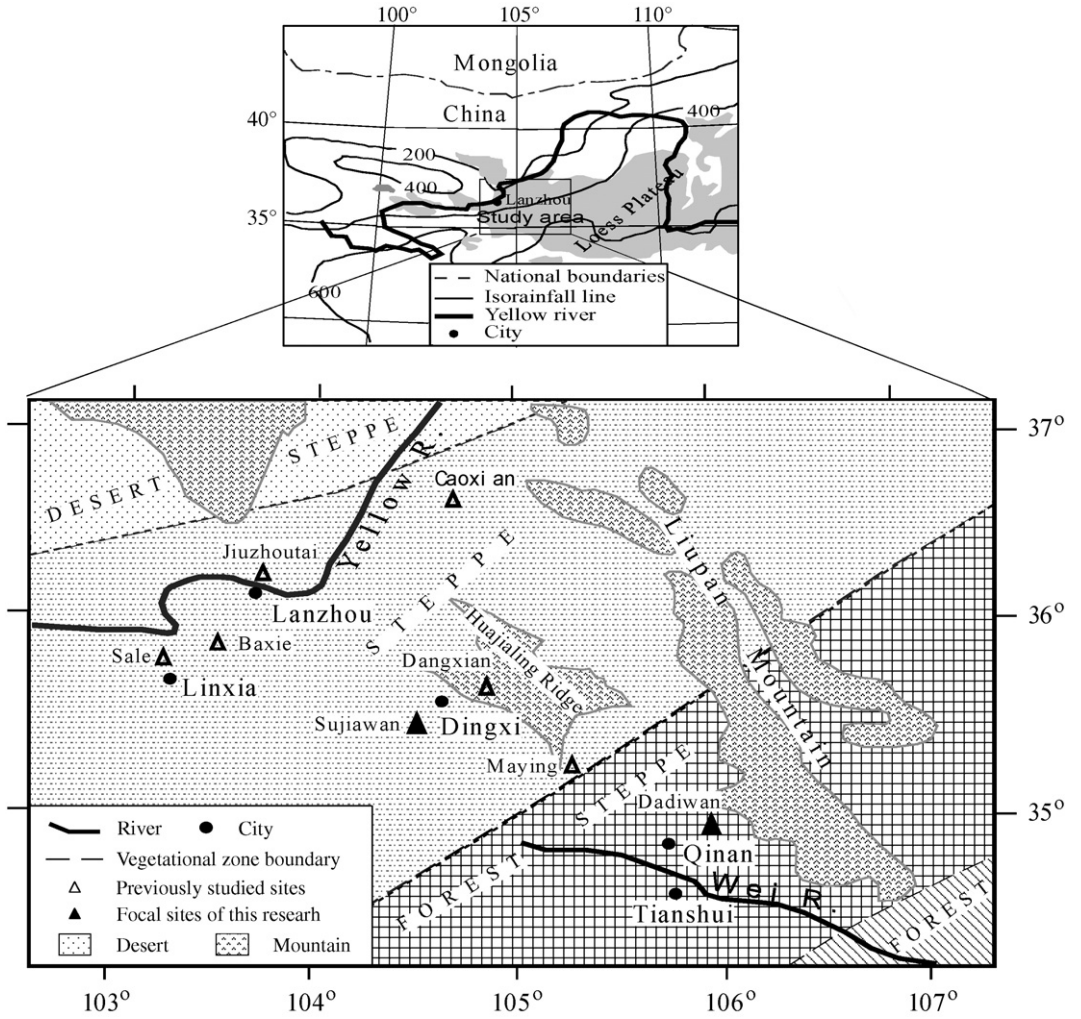

Fig. 1. Map showing the vegetation zones in the western part of the Chinese Loess Plateau. The locations of six reviewed sites (see Fig. 2A and B) and two focal sites (Sujiawan and Dadiwan) are also shown.

1.2. Modern physiographic settings

Because of the interaction between the winter and summer monsoons, there is SE–NW gradient of modern climate in the Chinese Loess Plateau (Li et al., 1988). That is, both mean annual temperature and precipitation decrease gradually from southeast (10 °C and 600 mm) to northwest (7 °C and 350 mm), whereas the aridity (ratio of evaporation to precipitation) increases from southeast (1.0) to northwest (3.0). The vegetation closely follows the aridity trend (Fig. 1): broadleaved deciduous forest in the southeastern corner, forest-steppe in the southeastern part, steppe in the northwestern part, and desert-steppe in the northwestern corner.

The western part of the Chinese Loess Plateau is notoriously vulnerable to environmental degradation due to four natural factors: steeply-sloped topography, fine-textured loessial soils, limited precipitation and most importantly, unique hydrogeomorphic conditions (Zhao et al., 2004). The unique hydrogeomorphic conditions refer to the fact that over 50% of precipitation occurs during July, August and September with over 60% of it being rainstorms whose intensity often exceeds the soil infiltration capacity. These factors suggest that not only is the limited precipitation unevenly distributed throughout the growing seasons but also gets little chance to infiltrate into the fine-textured loessial soils on the steeply-sloped topography. The extensive human removal of natural vegetation and the intensive human alterations of the soil hydrological properties (e.g., compaction) have further deteriorated the hydrogeomorphic conditions and consequently exacerbated the existing vulnerable ecological conditions. It is thus not a surprise to see that major rivers (except the Yellow River) have no or very little discharge for most time (approximately 300 days) of a year (Wu and Jiang, 1998), and croplands and treeless wastelands dominate the landscapes.

1.3. Previous studies of upland Holocene sequences

Although the loess/paleosol sequences in the Chinese Loess Plateau have been a scientific focal point of international Quaternary communities for the past 20–30 years, the top (Holocene) portions of these sequences did not get much attention because of difficulties in establishing high-resolution ^{14}C chronology based on bulk samples of thin Holocene sequences (Liu, 1987). However, the much thicker Holocene sequences (up to 5 m) along the northern border of the Loess Plateau have provided scientists with opportunities to overcome the chronological problem. That is, charcoal (the best AMS dating target) might have been preserved and soil humate might have survived from later contamination due to a higher rate of loess deposition. Consequently, the northern border of the Loess Plateau has become a Holocene-research hotspot (e.g., An et al., 1993; Gao et al., 1993; Zhou et al., 1991, 1996, 1999; An et al., 2000). Our research takes advantage of the relatively thick lowland Holocene sequences that occur as a series of swamp–wetland–eolian complexes in the western part of the Chinese Loess Plateau to obtain relatively high-resolution reconstructions of the Holocene climate changes based on more robust chronologies.

Before we discuss these lowland swamp–wetland–eolian complexes, we want to provide a brief review of six previously dated Holocene upland sequences in the western part of the Loess Plateau. Three of these relatively well-dated sequences are based on data from magnetic susceptibility and particle size (An et al., 1993; Chen et al., 1999; Wang, 2001), which are proxies for summer and winter monsoons, respectively (An et al., 1991; Maher, 1998; Chen et al., 2000). The paleoclimatic records from Caoxian (on flat-topped highland), Jiuzhoutai (on top of a loess hill near Lanzhou), and Baxie (on the third terrace of the Datong River—a major branch of the Yellow River) show that the climate started to ameliorate around 10,000–8000 ^{14}C years BP and deteriorated around 5000–3000 ^{14}C years BP (Fig. 2A). Three roughly-dated pollen sequences at Sale (Linxia) on Saleshan Mountain (Wang and Xu, 1988), Dangxian (Huining) on Huajialing Ridge (Tang et al., 1990), and Maying (Tongwei) on Huajialing Ridge (An, 2004) from mountainous areas (2000–2400 m above sea level) are summarized in Fig. 2B. The data show that the vegetation changed from glacial loess-associated steppe to Holocene paleosol-associated forest (9300–5650 ^{14}C years BP), and then deteriorated afterward in the Saleshan Mountain. The vegetation in the Huajialing Ridge changed from glacial loess-associated steppe to Holocene paleosol-associated forest-steppe (from 6510+ ^{14}C years BP to 3780+ ^{14}C years BP). It should be particularly noted that the early–middle Holocene paleosol is well-preserved in the flat-topped Huajialing Mountains (see Fig. 1) and also on the flat-topped highlands (e.g., Caoxian). It survived from slope erosion only on gentle tops of loess hills (e.g., Jiuzhoutai) and is well preserved on valley terraces. The paleosol should have formed synchronously in the western part of the Loess Plateau although the chronologies do not provide a neat age bracket for the paleosol formation. Considering the inherently large errors resulting from the mixing processes of time-diachronous organic matter in the aforementioned six upland sequences, 10,000–8000 ^{14}C

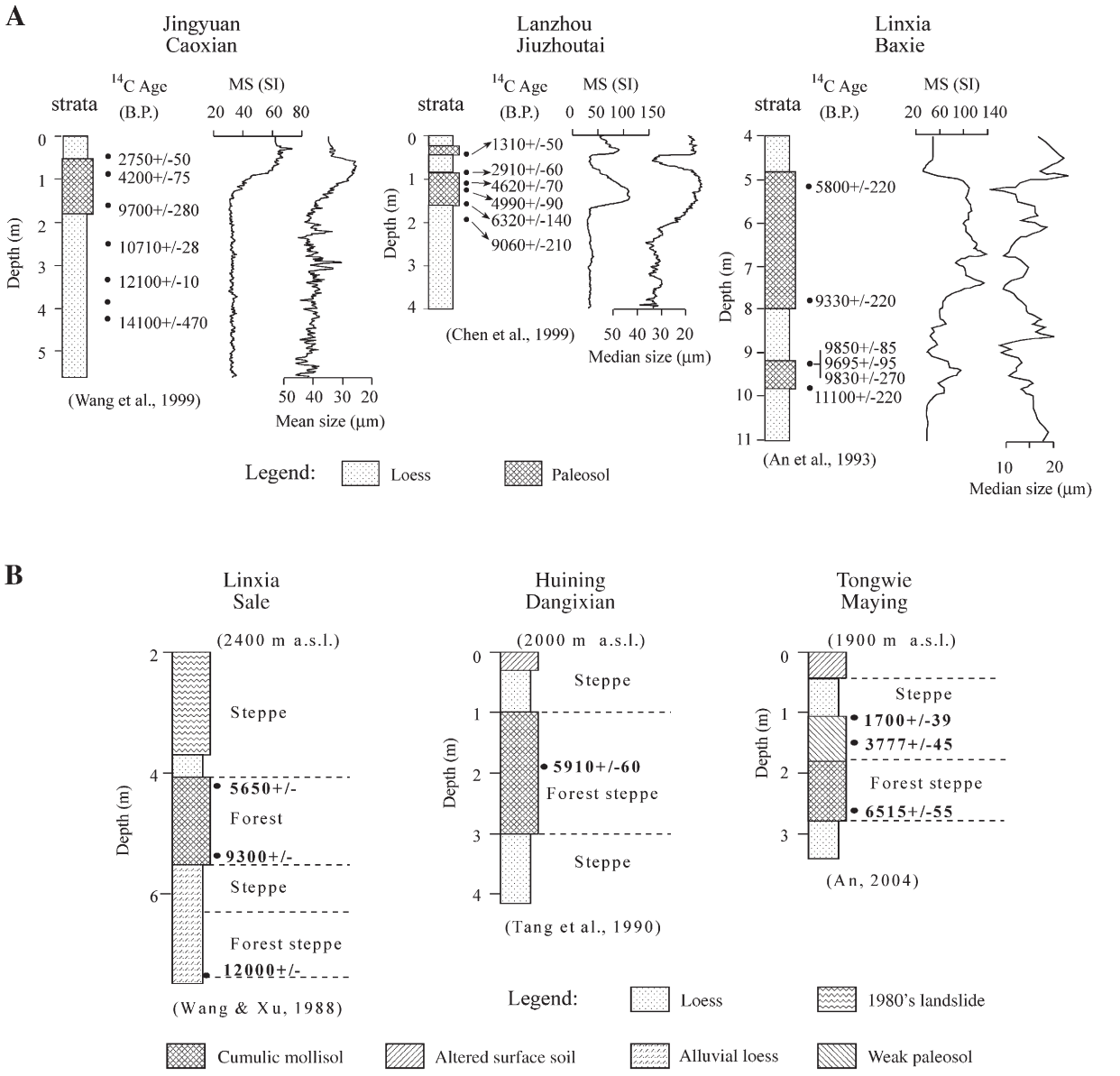

Fig. 2. (A) A summary of three previously well-dated upland Holocene sequences (Caoxian, Jiuzhoutai, Baxie) and the proxy data (magnetic susceptibility and particle size) within the study area. (B) A summary of three previously roughly-dated upland Holocene pollen sequences (Sale, Dangxian, Maying) within the study area.

years BP and 5000–3000 ^{14}C years BP can be taken as the approximate bracket ages of the upland paleosols in the western part of the Loess Plateau.

2. Field work and laboratory methods

2.1. Field survey of valley Holocene sequences

In contrast to the above-described upland Holocene sequence, the valley Holocene sequence in the western part of the Chinese Loess Plateau consists of an upper loess–soil complex and a lower wetland–swamp complex (see inset photo 1 in Fig. 3). The lower wetland–swamp complex stands out so striking in this semiarid environment that the senior author (Feng) and his colleagues recently (2000–2003) conducted 10 fieldtrips to survey the extent of the complex for reconstructing the paleo-environment. Fig. 3 shows the field-surveyed distribution of the lower complex. It can be concluded, based on the surveyed geomorphic settings of the complex, that the actual extent of the lower complex is much larger. It should also be noted

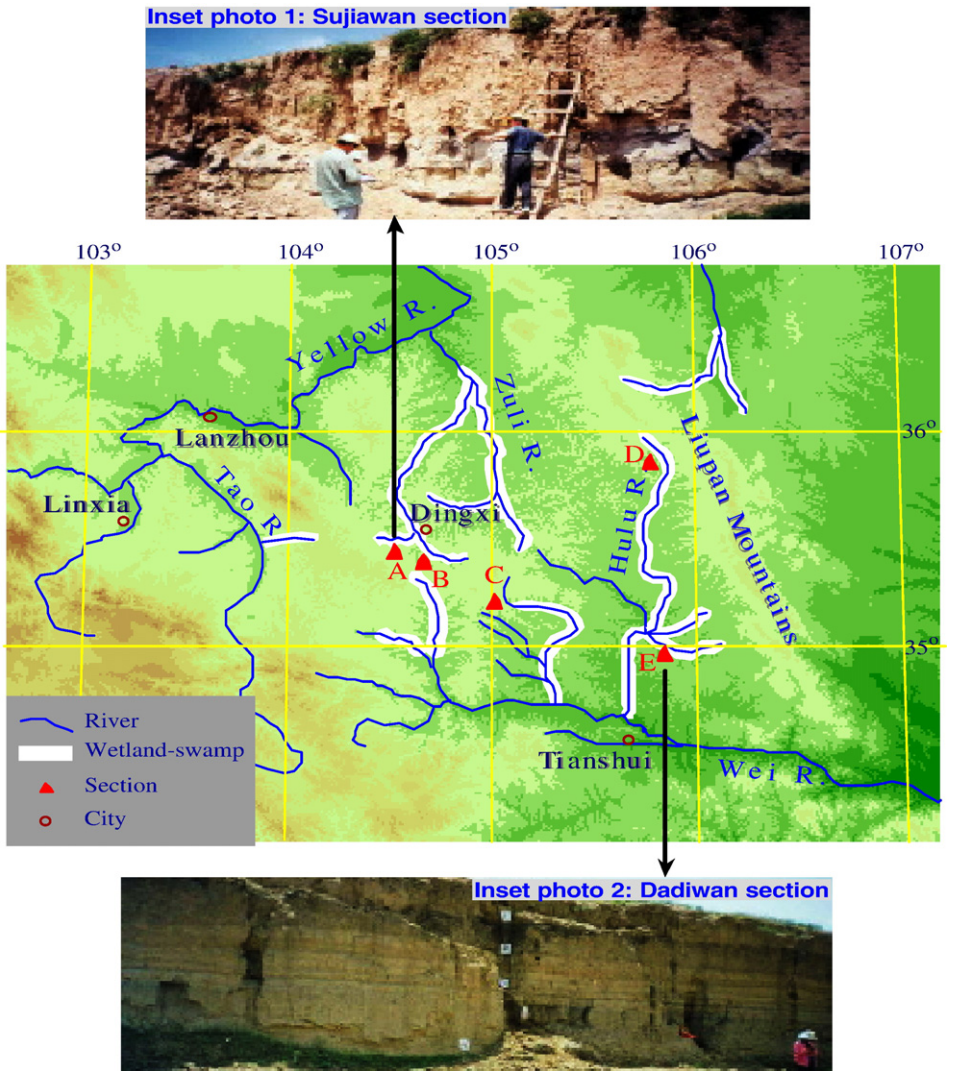

Fig. 3. Field-surveyed distribution of the wetland–swamp facies formed between 8880 and 3800 ^{14}C years BP and the locations of five dated valley Holocene sequences in the study area. Inset photo 1: Sujiawan section, and inset photo 2: Dadiwan section.

that the lower complex is thickened by fluvial aggradations and expressed as a wetland–swamp–fluvial complex in the major branch rivers (e.g., at Dadiwan; see inset photo 2 in Fig. 3).

2.2. Valley Holocene chronosequences

Fig. 4 shows five representative sections that were AMS ^{14}C dated (see Fig. 3 for site locations). The lower wetland–swamp complex at four of these five sections (A: Sujiawan; B: Dingxi; C: Maying; and D: Shanjiaji) is a greyish-blue clayey silt unit. Aquatic mollusks comprise much of the complex, and carbonate powder and half-decomposed organic matter are readily visible. This complex is well bracketed by two AMS dates at the Sujiawan section: 8885±55 and 3805±45 ^{14}C years BP. All the dates of the complex from other sections fall within this age bracket (Feng et al., 2004). The upper loess–soil complex covers the dust-depositing and soil-forming history of the past ~4000 years. The stratigraphically traceable equivalent to the lower wetland–swamp complex in the major branch rivers is a fluvially aggraded and thickened wetland–swamp–fluvial complex, which is well expressed at the Dadiwan section (see Section E in Fig. 4).

2.3. Laboratory methods

We have conducted systematic laboratory analyses on the samples taken from two representative sections,

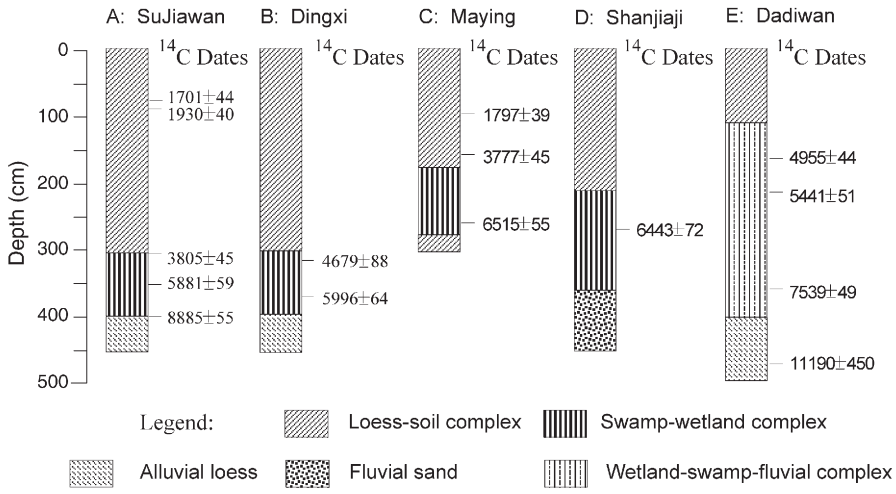

Fig. 4. Five recently dated valley Holocene sequences in the study area. Sections A (Sujiawan), B (Dingxi), C (Maying), and D (Shanjiaji) are typical in the major valleys and Section E (Dadiwan) is typical in major branch valleys.

Sujiawan and Dadiwan, to obtain proxy data for reconstructing the Holocene history of the vegetation variations and the associated environmental changes. Sampling intervals were 2 cm in the lower portion (300–400 cm deep), 5 cm in the upper portion (50–300 cm deep) and 10 cm in the top 50 cm within the Sujiawan section. All the samples were taken at 2-cm intervals within the Dadiwan section. The carbonate concentration was measured using a Bascomb Calcimeter and the organic matter with the titration method (Singer and Janitzky, 1987). The particle size of bulk samples was measured using a Malvern laser diffraction particle size analyzer and snails were identified with reference to resource manual. For pollen analysis, the sediments were treated with HCl (10%), NaOH (10%) and HF (36%). Exotic *Lycopodium* tablets were added for calculation of pollen concentration (Moore et al., 1991; Wang et al., 1995). Over 200 pollen grains were identified in all of the samples except for five samples in which only 100–200 pollen grains were identified. A total of more than 60 pollen and spore types were distinguished.

3. Results and discussions

The two representative sections can compensate for each other's shortcomings. That is, the lower wetland–swamp complex at the Sujiawan section is well age-constrained but the resolution is compromised (only 1 m thick). The chronology of the equivalent to the wetland–swamp complex at the Dadiwan section is not satisfactory due to fluvial aggradation-resulted local age reversals, but this fluvial aggradation-thickened complex (3 m thick) provides a higher stratigraphic resolution. In addition, the upper loess–soil complex at the Dadiwan section seems incomplete or severely disturbed, but the upper complex at the Sujiawan section appears to contain a complete record of the history of the late Holocene vegetation variations and the associated environmental changes.

3.1. Modern vegetation and pollen representation

To reconstruct the Holocene vegetation variations and the associated environmental changes, we need to understand the relationships between modern pollen deposition and its associated vegetation. The following is a brief summary of the published descriptions of modern pollen–vegetation relationships pertinent to the western part of the Loess Plateau.

3.1.1. Temperate deciduous forest

The dominant tree taxa include *Quercus*, *Betula*, *Alnus*, *Acer*, *Ulmus*, *Populus* and *Pinus*. The pollen spectra of the surface soil are dominated by the deciduous forest taxa (9.0–50.0%), *Pinus* (5.9–54.6%) and *Artemisia* (3.9–58.8%), accompanied by Gramineae (1.1–10.0%) and Chenopodiaceae (1.0–11.5%) (Wang et al., 1996; Zhao et al., 1998; Xu et al., 2000).

3.1.2. Temperate steppe forest

The dominant plant taxa are *Pinus*, *Quercus*, *Betula*, *Ulmus*, *Populus*, Gramineae, *Artemisia*, Leguminosae, *Lespedeza* and *Caragana*. The modern pollen spectra are co-dominated by the herb component (20.0–80.0%) and the arboreal component (15.0–40.0%). The arboreal

component includes *Pinus* (5.1–42.2%), *Quercus* (1.1–11.9%) and *Betula* (0.6–17.0%), and the herb component includes *Artemisia* (20.8–50.6%), Chenopodiaceae (6–15.0%), and Gramineae (2.1–8.6%) (Yan and Xu, 1989; Tong et al., 1996; Li, 1998; Liu et al., 1999; Ma, 2004; Ma et al., 2004).

3.1.3. Temperate steppe

The modern pollen spectra are dominated by the herb component (62.0–93.0%) with a minor *Pinus*-dominated arboreal component (7.0–28.0%). The herb component includes *Artemisia* (36.5–80.0%), Compositae (10–20%), Chenopodiaceae (14.9–46.6%), and Gramineae (2.2–10.0%) (Li, 1998; Liu et al., 1999).

3.1.4. Temperate desert steppe

The high percentages of *Artemisia* (20.6–55.8%) and Chenopodiaceae (23.1–48.6%) properly represent the dominance of these two herbaceous taxa, whereas *Stipa* (Gramineae) is under-represented. The pollen percentage of Gramineae, as well as the percentages of the arboreal component, is below 10% (Yan and Xu, 1989; Li, 1998).

It should be added that major coniferous trees (e.g., *Pinus*, *Abies* and *Picea*) are normally over-represented (Ma et al., 2004) and *Ulmus* is under-represented in the modern pollen spectra (Li, 1998), while *Quercus* is properly represented (Zhao et al., 1998). For example, large patches of *Ulmus* trees may only yield <10% of *Ulmus* pollen in the surface samples. On the other hand, even up to 30% of coniferous tree pollen cannot be interpreted as a reflection of local existence of forest or forest-steppe if other tree taxa are lacking (Li, 1998; Ma et al., 2004).

3.2. Proxy data at the Sujiawan section

3.2.1. Detailed chronosequence

The Holocene sequence at the Sujiawan section (104°31′22″E, 35°32′20″N; 1950 m a.s.l.) consists of two complexes: an upper loess–soil complex and a lower wetland–swamp complex. The lower complex is a greyish-blue clayey silt unit (about 1 m thick). Nearly horizontal sub-layers were evidently affected by bioturbation. Aquatic mollusks comprise much of the layer. We have interpreted the layer as a wetland–swamp complex and four charcoal AMS dates well define the period of its deposition. That is, the lower complex was formed between 8880 and 3800 ^{14}C years BP (Fig. 5 and Table 1). Below the wetland–swamp complex is a

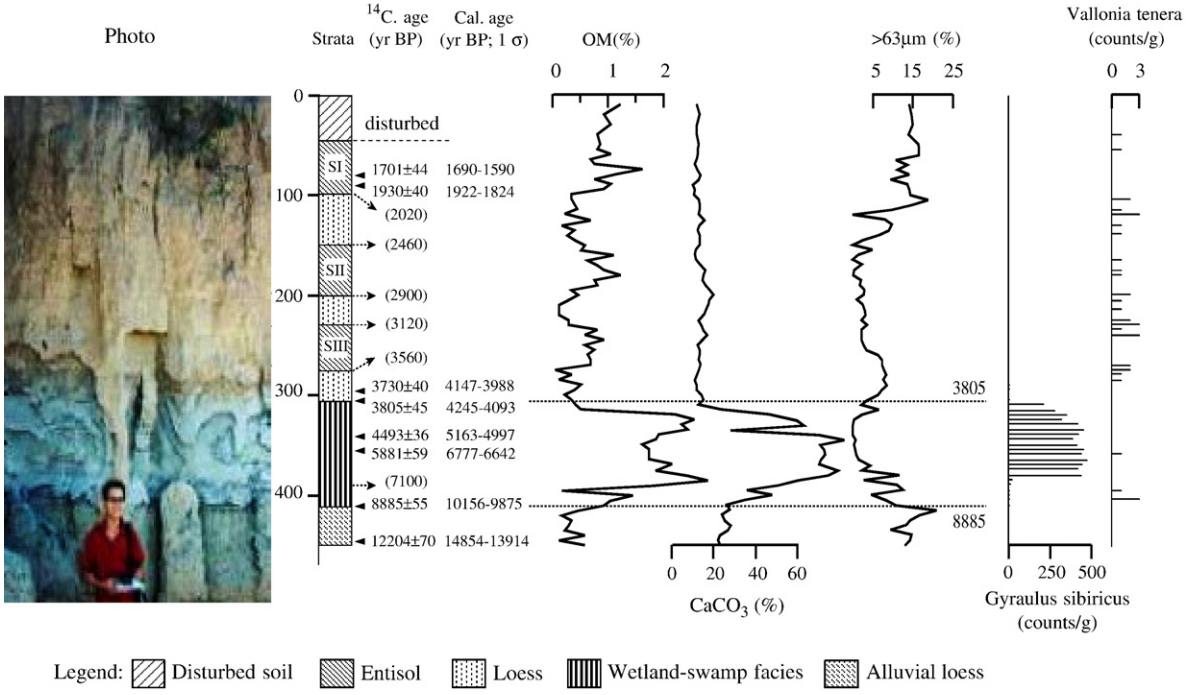

Fig. 5. Sujiawan section: photo, pedo- and lithostratigraphy, AMS dates and interpolated ages (parenthesized ages). The proxy data include organic matter content (OM), carbonate concentration ($CaCO_3$), percentage of >63 μm fraction (>63 μm), counts of aquatic mollusk (*Gyraulus sibiricus*) and terrestrial mollusk (*Vallonia tenera*).

Table 1
AMS dates of the Holocene sequence at the Sujiawan section (AA samples: dated at the NSF AMS Facility and Beta samples: at Beta Analytic Inc.)

Sample no.	Lab no.	Depth (cm)	Dated material	^{14}C age	Cal. age (1σ)
DXSJW80	AA56728	80–81	Bone	1701±44	1690–1590
SJ90	Beta181611	90–91	Charcoal	1930±40	1922–1824
SJ295	Beta181612	295–296	Charcoal	3730±40	4147–3988
DXSJW305	AA44885	305–306	Charcoal	3805±45	4245–4093
DXSJW340	AA56711	340–341	Soil humate	4493±36	5163–4997
DXSJW455	AA44886T	355–356	Charcoal	5851±50	6777–6642
DXSJW410	AA44886	410–411	Charcoal	8885±55	10,156–9875
DXSJW445	AA56712	445–446	Soil humate	12,204±70	14,854–13,914

strongly gleyed loess unit and a charcoal AMS date was obtained at the depth of 445 cm (12,204±70 ^{14}C years BP). Fig. 5 and Table 1 also include the calibrated ages using INTCAL98 (Stuiver et al., 1998).

The upper complex is composed of three Entisols with organic matter-enriched A horizons. The A horizons are characterized by slightly more compaction with observable granular structures and by a darker colour with more rootlet channels than the interbedding loess units. Three charcoal AMS dates were obtained at the depths of 80 cm (1701±44 ^{14}C years BP), 90 cm (1930±40 ^{14}C years BP), and 295 cm (3730±40 ^{14}C years BP). Assuming that the depositional rate was relatively constant from 3805±45 to 1930±40 ^{14}C years BP, based on the fact that the percentage of the >63 μm fraction varies very little from 305 cm to 90 cm (see Fig. 5), we obtained an age–depth conversion (i.e., 1 cm=8.8 years). The interpolated bracket ages are 3560 and 3120 ^{14}C years BP for the Entisol SIII and 2900 and 2460 ^{14}C years BP for the Entisol SII. The interpolated bottom age of the Entisol SI (at the depth of 100 cm) is 2020 ^{14}C years BP (the interpolated ages are parenthesized in Fig. 5).

3.2.2. Non-pollen proxy data

The wetland–swamp complex is characterized by a high content of organic matter (up to 2.5%) and a high concentration of carbonate (up to 70%). The complex is finer than other stratigraphic units, as indicated by the percentage of the coarse (>63 μm) fraction. The extremely high counts of aquatic snails, *Gyraulus sibiricus* (up to 250 counts/g), and the absence of terrestrial snails (*Vallonia tenera*) strongly suggest that this unit is a wetland–swamp facies (Fig. 5). It is notable that the wetland–swamp condition started more or less gradually around 8880 ^{14}C years BP and ended abruptly around 3800 ^{14}C years BP, as indicated by all proxy data in Fig. 5.

The terrestrial snail-rich (*V. tenera*) upper loess–soil complex is further divided into three Entisol units as observed in field and indicated by the organic matter content. The percentage of the >63 μm fraction (Fig. 5) does not distinguish the organic matter-enriched Entisol A horizons from the interbedding loess units, implying that the eolian flux rate was relatively constant from 3560 to 2020 ^{14}C years BP, although organic matter content suggests that the accumulation rates of organic matter were apparently higher during the soil-forming periods of SIII (3560–3120 ^{14}C years BP) and SII (2900–2460 ^{14}C years BP) than during the loess-depositing intervals (3120–2900 ^{14}C years BP, and 2460–2020 ^{14}C years BP). The SI (100–50 cm) is characterized by a high percentage of >63 μm fraction and also by a high percentage of organic matter content, probably suggesting that the SI was formed under a dusty and yet a denser vegetation condition.

3.2.3. Pollen data

The Sujiawan section is divided into six units based on the pollen assemblages: A, B, C, D, E, and F from the top to the bottom (Fig. 6).

3.2.3.1. Zone F (450–410 cm; 12,200–8880 ^{14}C years BP). This gleyed loess unit underlying the wetland–swamp complex is dominated by the herb component (*Artemisia*, Compositae, and Gramineae) with an extremely low pollen concentration, suggesting a desert-steppe landscape during the late glacial.

3.2.3.2. Zone E (410–340 cm; 8880–4490 ^{14}C years BP). The lower portion of the wetland–swamp complex is dominated by coniferous tree component (e.g., *Pinus*, *Abies*, *Picea*, *Tsuga*), accompanied by a considerable amount of deciduous tree pollen (e.g., *Betula*, *Juglans*, *Ulmus* and *Celtis*) and herb pollen (Gramineae, Compositae, and *Artemisia*). It is also noticeable that *Typha* and Cyperaceae are detected in every sample. Both the pollen concentration (up to 8000 grains/g) and the percentage of the tree–shrub component (up to 80%), being the highest in the entire

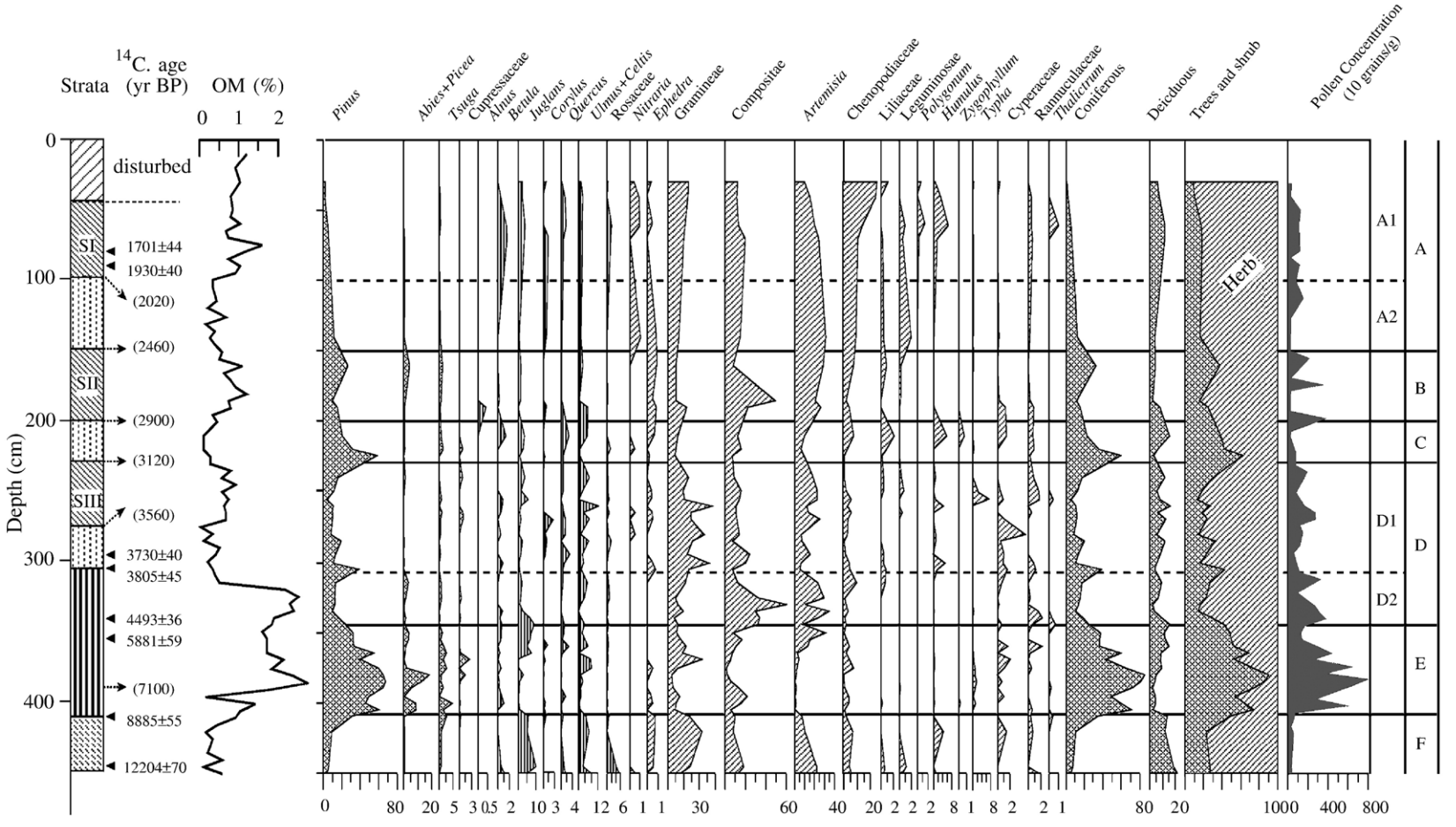

Fig. 6. Pollen diagrams and pollen biostratigraphic zones at the Sujiawan section with reference to stratigraphy and chronology.

section, suggest the existence of a temperate forest at least in valleys or/and in nearby highlands during the early part (8880–4490 ^{14}C years BP) of the wetland–swamp facies-forming period (8880–3800 ^{14}C years BP). It should also be noted that the vegetation was the densest (i.e., achieved highest pollen concentration) between 7100 ^{14}C years BP (385 cm) and 4490 ^{14}C years BP (340 cm), the former age (7100 ^{14}C years BP) being linearly interpolated between two adjacent dates (8885 and 5881 ^{14}C years BP).

3.2.3.3. Zone D (340–230 cm; 4490–3120 ^{14}C years BP). The pollen spectra are dominated by the herb component with relatively low percentages (20–50%) of the tree–shrub component and relatively low pollen concentrations (1000–3000 grains/g), representing a temperate steppe landscape according to the above-described modern analogue. Zone D can be further divided into two subzones: D2 and D1. Subzone D2 (340–305 cm; 4490–3800 ^{14}C years BP) represents a Compositae-dominated steppe landscape and Subzone D1 (305–230 cm; 3800–3120 ^{14}C years BP) represents a Gramineae-dominated steppe landscape.

3.2.3.4. Zone C (230–200 cm; 3120–2900 ^{14}C years BP). Although the *Pinus* pollen percentage is rather high (20–40%), the extremely low pollen concentration (200–1000 grains/g) and very low abundance of deciduous tree pollen suggest that the pollen assemblage probably represents a transitional landscape between a steppe and a desert-steppe.

3.2.3.5. Zone B (200–150 cm; 2900–2460 ^{14}C years BP). This zone is the paleosol SII and characterized by a moderate peak in *Pinus* (up to 30%). Compositae (up to 50%) dominates the herb component. It is also quite noticeable that *Artemisia* and Chenopodiaceae start to increase upward and the pollen concentration fluctuates around a moderate mean. The assemblage probably represents a steppe landscape.

3.2.3.6. Zone A (150–50 cm; 2460 to ~1000? ^{14}C years BP). This zone includes the paleosol SI (100–50 cm) and the underlying loess unit (150–100 cm) and is characterized by a consistently low pollen concentration and by an extremely high percentage (about 80%) of herbs. This zone can be further divided into two subzones: A2 and A1. Subzone A2 (loess unit; 150–100 cm; 2460–2020 ^{14}C years BP) contains more *Nitraria*, *Ephedra* and *Artemisia* than Subzone A1 (paleosol SI; 100–50 cm; 2020 to ~1000 ^{14}C years BP). The former (Subzone A2) may represent a desert-steppe landscape and the latter (Subzone A1) may represent a steppe landscape.

3.3. Proxy data at the Dadiwan section

3.3.1. Detailed chronosequence

The Dadiwan section (35°00′47.3″N, 105°54′53.3″E, 1471 m a.s.l.) is a stratigraphically traceable (we actually traced) equivalent to the wetland–swamp complex of the Sujiawan section. It is a wetland–swamp–fluvial complex that is overlain by a surface Mollisol (0–115 cm) with an A–B–C profile and underlain by a fluvially-altered loess unit (450–500 cm). The wetland–swamp–fluvial complex (115–450 cm) includes three sub-units: (1) a pedogenically-altered wetland-facies upper layer (115–170 cm), (2) a wetland–fluvial-facies middle layer (170–355 cm), and (3) a wetland–swamp-facies bottom layer (355–450 cm). The middle layer (170–355 cm) contains four wetland and fluvial alternating couplets. Local reversals of the ^{14}C dates are relatively well documented at this section. For example, a charcoal date (5136±45 ^{14}C years BP) at the upper position (131–132 cm) is older than two charcoal dates (4955±44 and 5441±51 ^{14}C years BP) at the lower positions (170–171 cm and 190–191 cm) in the upper portion of the complex. Four charcoal dates are completely reversed in the lower portion of the complex (285–356 cm) and an age reversal (11,850 ^{14}C years BP at 460 cm and 11,190 ^{14}C years BP at 472 cm) also occurs in the fluvially-altered loess at the bottom of the section.

Our interpretation of these systematic age reversals is that the major flooding-related fluvial processes eroded older charcoals from the uplands and re-deposited them on the floodplains. In each of the three reversed sequences (130–192 cm, 285–356 cm, and 460–474 cm), the younger dates marked with calibrated ages both in Fig. 7 and Table 2 are considered to represent the real ages of then-floodplain surfaces. It should be noted that one snail age (10,279 ^{14}C years BP at 240–242 cm) and one pollen age (14,622 ^{14}C years BP at 385–387 cm) are anomalously too old, and two soil-humate dates (5371±50 ^{14}C years BP at 100–102 cm and 9007±50 ^{14}C years BP at 332–334 cm) are also somewhat too old in comparison with the charcoal dates (see Table 2). These four dates (marked with * in Table 2) are not plotted in Fig. 7.

It should be particularly noted that although the local age reversals are obvious, the overall chronosequence is reasonably well supported by those charcoal dates. Specifically, the upper portion of the wetland–swamp–fluvial complex (130–190 cm) was formed

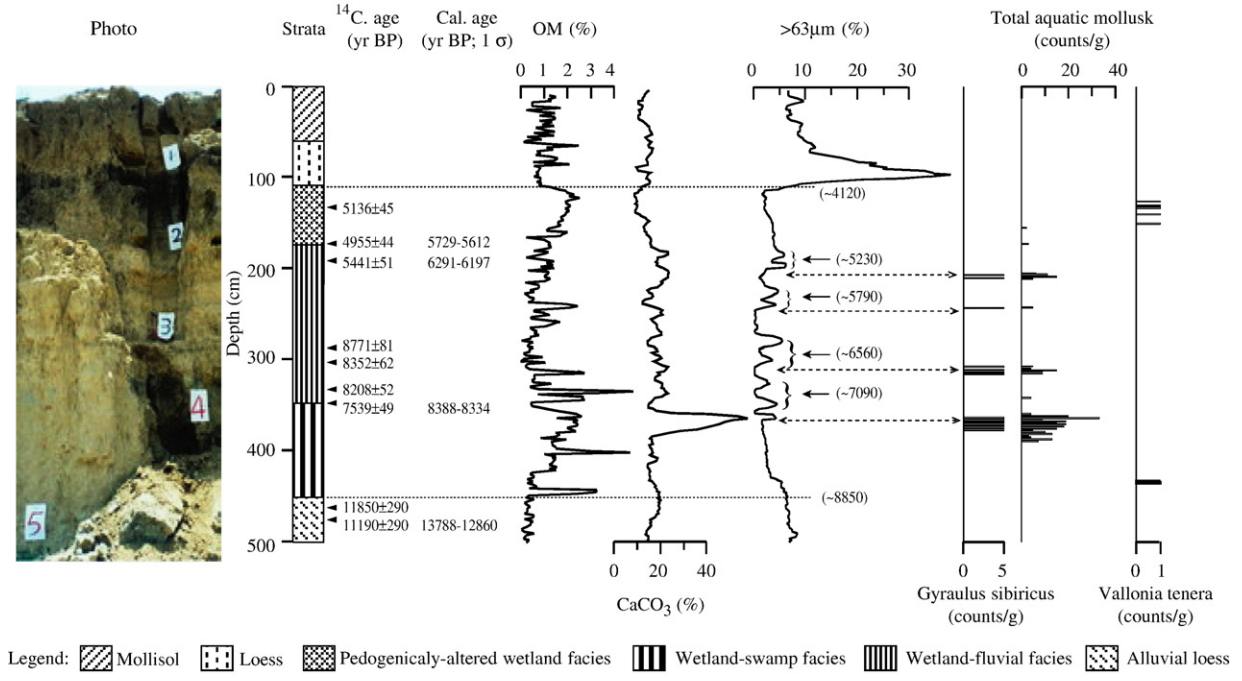

Fig. 7. Dadiwan section: photo, pedo- and lithostratigraphy, AMS dates and interpolated ages (parenthesized ages). The proxy data include organic matter content (OM), carbonate concentration ($CaCO_3$), percentage of >63 μm fraction (>63 μm), counts of aquatic mollusk (*Gyraulus sibiricus*), total aquatic mollusk, and terrestrial mollusk (*Vallonia tenera*).

around 5000 ^{14}C years BP and the lower portion (285–330 cm) around 8000 ^{14}C years BP. Here, we use two charcoal dates (4955±44 ^{14}C years BP at 170 cm and 7539±49 ^{14}C years BP at 355 cm) to linearly interpolate and extrapolate the ages of the starting point (115 cm) and the ending point (450 cm) of the wetland–swamp–fluvial complex. We also interpolated the ages of the four field-observed and photo-displayed (Fig. 7) flooding events (at ~190 cm, ~230 cm, ~285 cm, and ~330 cm). This linear interpolation and extrapolation is based on two observations: (1) the overall trend of the >63 μm fraction within the wetland–swamp–fluvial complex (115–450 cm) does not vary very much, especially considering the fact that the small peaks of the >63 μm fraction were generated by short-lived flooding-related fluvial processes; and

Table 2
AMS dates of the Dadiwan Holocene sequence (all dated at the NSF AMS Facility)

Sample no.	Lab no.	Depth (cm)	Dated material	^{14}C age	Cal. age (1σ)
DDW2	AA43792	131–132	Charcoal	5136±45	
DDW170	AA44889	170–171	Charcoal	4955±44	5729–5612
DDW190	AA44887	190–191	Charcoal	5441±51	6291–6197
DDW5	AA43795	285–286	Charcoal	8771±81	
DDW6	AA43796	300–301	Charcoal	8352±62	
DDW7	AA43797	330–331	Charcoal	8208±52	
DDW8	AA43798	355–356	Charcoal	7539±49	8388–8334
DDW460	AA43791	460–461	Charcoal	11,850±290	
DDW472	AA49110	472–473	Charcoal	11,190±290	13,788–12,860
DDW1	AA43791	100–102	Soil humate	5371±50	*
DDW4	AA43794	240–242	Snails	10,279±74	*
DDW332	AA49112	332–334	Soil humate	9007±50	*
DDW9	AA43799	385–387	Pollen	14,622±97	*

(2) the charcoal samples for these two dates used for the linear interpolation and extrapolation (4955±44 ^{14}C years BP and 7539±49 ^{14}C years BP) exactly bracket the fluvial process-dominated wetland–fluvial-facies middle layer (170–355 cm). That is, the upper bracket age (4955±44 ^{14}C years BP) was obtained at the bottom of the pedogenically-altered wetland-facies (non-fluvial) upper layer (at 170 cm) that immediately overlies the wetland–fluvial-facies middle layer (170–355 cm), and the lower bracket age (7539±49 ^{14}C years BP) was obtained at the top of the wetland–swamp (non-fluvial) bottom layer (at 355 cm) that immediately underlies the wetland–fluvial-facies middle layer (170–355 cm). This implies that these samples were not reworked by later flooding-related fluvial processes. The calculated age–depth conversion is: 1 cm=14 years and the linearly interpolated and extrapolated bracket ages for the wetland–swamp–fluvial complex are 4120 ^{14}C years BP (at 115 cm) and 8850 ^{14}C years BP (at 450 cm). The interpolated ages for those four flooding events are: ~5230 ^{14}C years BP (at ~190 cm that was actually dated at 5441±51 ^{14}C years BP), ~5790 ^{14}C years BP (at ~230 cm), ~6560 ^{14}C years BP (at ~285 cm), and ~7090 ^{14}C years BP (at ~330 cm), each of them being predated by a depositional interval of aquatic snail-rich wetland facies (see Fig. 7). It should be stressed that the bracket ages of the wetland–swamp–fluvial complex (4120 ^{14}C years BP and 8850 ^{14}C years BP) at the Dadiwan section are in reasonable agreement with the bracket ages of its equivalent (i.e., wetland–swamp complex) at the well-dated Sujiawan section (3805 ^{14}C years BP and 8885 ^{14}C years BP), suggesting that these linearly interpolated and extrapolated ages are acceptable again considering the error bars and the calibration-related uncertainties of the dates.

3.3.2. Non-pollen proxy data

The aquatic snail-rich wetland–swamp–fluvial complex (115–450 cm) is characterized by relatively high carbonate concentrations. The organic matter content is relatively high in the pedogenically-altered wetland-facies upper layer (115–170 cm) and in the wetland–swamp-facies bottom layer (355 to 450 cm). Again, the percentage of the >63 μm fraction indicates that the wetland–swamp condition started gradually from the top (at the depth of 450 cm) of late glacial alluvial loess and ended abruptly at the inferred age of 4120 ^{14}C years BP (i.e., at the depth of 115 cm). It is notable that the type aquatic species, *G. sibiricus*, well marks four periods of land-surface stability as indicated by wetland–swamp depositional facies (see photo in Fig. 7), each of which immediately predated a major flooding event as indicated by the percentage of the >63 μm fraction. The surface Mollisol with a complete A–B–C profile (0–115 cm) is not dated for lack of charcoal, and the soil-forming processes (e.g., bioturbation and clay translocation) in the A and B horizons made the top 50 cm unsuitable for a high-resolution reconstruction.

3.3.3. Pollen data

The section can be divided into six units based on the pollen assemblages: A B, C, D, E, and F from the top to the bottom (Fig. 8).

3.3.3.1. Zone F (500–450 cm; ~11,190±290 ^{14}C years BP). The pollen spectra are overwhelmingly dominated by herbs (up to 90%) with a very low pollen concentration (100–500 grains/g). The herbs are Compositae (20–60%) and *Artemisia* (30–40%) with detectable amounts of *Crepis*, *Humulus*, and *Zygophyllum*. *Pinus* pollen was also found but the percentage is extremely low (1–5%). This assemblage most likely represents a steppe landscape or a desert-steppe landscape.

3.3.3.2. Zone E (450–355 cm; 8850–7540 ^{14}C years BP). The dominant herb component includes Compositae (up to 40%) and *Artemisia* (up to 35%). But, besides *Pinus* pollen, other tree and shrub taxa (5–30%) start their appearance (e.g., *Sabina*, Cupressaceae, *Juglans*, *Quercus*, *Ulmus*, Rosaceae) with *Crepis* and *Zygophyllum* being as high as 10%. The pollen concentration fluctuates between 300 and 1500 grains/g. The assemblage probably represents a forest-steppe landscape.

3.3.3.3. Zone D (355–170 cm; 7540–4950 ^{14}C years BP). This zone can be further divided into three subzones: D3, D2, and D1.

Subzone D3 (355–285 cm; 7540 to ~6560 ^{14}C years BP) is characterized by the dominance of coniferous tree taxa (30–80%) including *Pinus* (20–80%), *Picea* and *Abies* (5–15%), *Tsuga* (up to 5%) and *Sabina* (5–20%). Although the percentage of tree–shrub pollen reaches the highest in the entire section, the pollen concentration remains relatively low (500–1500 grains/g). It is most likely that a *Pinus*-dominated forest occupied the area or at least was proximate to the site.

Subzone D2 (285–230 cm; 6560–5790 ^{14}C years BP) has the highest pollen concentration (up to 6500 grains/g) and the highest deciduous tree pollen percentage (up to 40%) with a dramatic appearance of

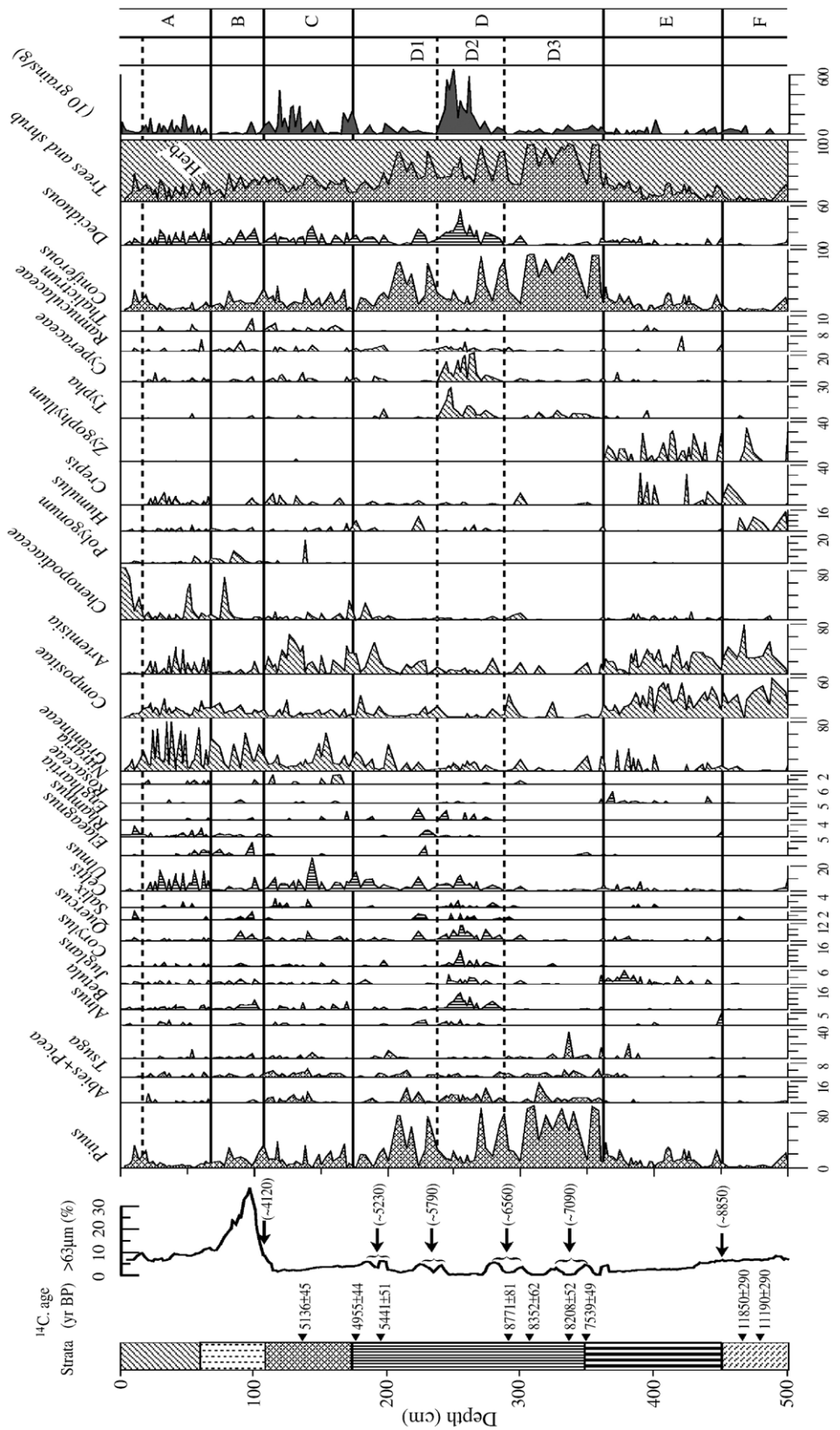

Fig. 8. Pollen diagrams and pollen biostratigraphic zones at the Dadiwan section with reference to stratigraphy and chronology.

Typha (up to 30%) and Cyperaceae (up to 30%). The pollen spectra are co-dominated by the tree–shrub component and the herb component. This pollen assemblage represents a temperate deciduous forest landscape with maximum density and diversity during the entire Holocene period.

Subzone D1 (230–170 cm; 5790–4950 ^{14}C years BP) has a relatively low pollen concentration (500–1500 grains/g) and both the percentage of the herb pollen and the percentage of coniferous tree pollen (especially *Pinus*) increase at the expense of other tree pollen, whereas *Typha* and Cyperaceae nearly completely disappear. The assemblage probably represents a *Pinus*-dominated forest-steppe landscape.

3.3.3.4. Zone C (170–115 cm; 4950–4120 ^{14}C years BP). The fluctuating high pollen concentration values (up to 4000 grains/g) and the proportional shares of the pollen spectra by the tree–shrub component (30–40%) and the herb component (60–70%) indicate that this pedogenically-altered wetland-facies layer was formed under the second densest vegetation cover in the entire section. The increased *Ulmus* pollen percentage and decreased *Pinus* pollen percentage, along with higher Gramineae (10–60%) and *Artemisia* (5–30%) percentages and lower Compositae (5–10%) and Chenopodiaceae (5–10%) percentages, suggest an *Ulmus*-dominated forest-steppe landscape.

3.3.3.5. Zone B (115–55 cm; 4120 to ~2000+? ^{14}C years BP). This coarse loess unit or C horizon of the surface Mollisol contains predominantly herb pollen (up to 70%). *Pinus* (10–25%) and *Ulmus* (5–10%) are the predominant tree taxa with detectable amounts of other tree pollen and some shrub pollen (e.g., *Nitraria*). Although the assemblage looks like a representative of a forest-steppe landscape, the extremely low pollen concentration (200–300 gains/g) seems to suggest a steppe landscape. It should be particularly noted that the upper age (2000+? ^{14}C years BP at the depth of 50 cm) is inferred based on the reported upland Holocene sequences in which 2000 ^{14}C years BP marks the beginning of the most recent major climatic amelioration of the Holocene in the Chinese Loess Plateau (Liu, 1987).

3.3.3.6. Zone A (55–0 cm; ~2000+?–0? ^{14}C years BP). The pollen concentration in this surface Mollisol A and B horizons is relatively high (1000–2500 grains/g) and the dominant herb component is accompanied with *Ulmus* (up to 20%), probably representing an *Ulmus*-dominated forest-steppe landscape.

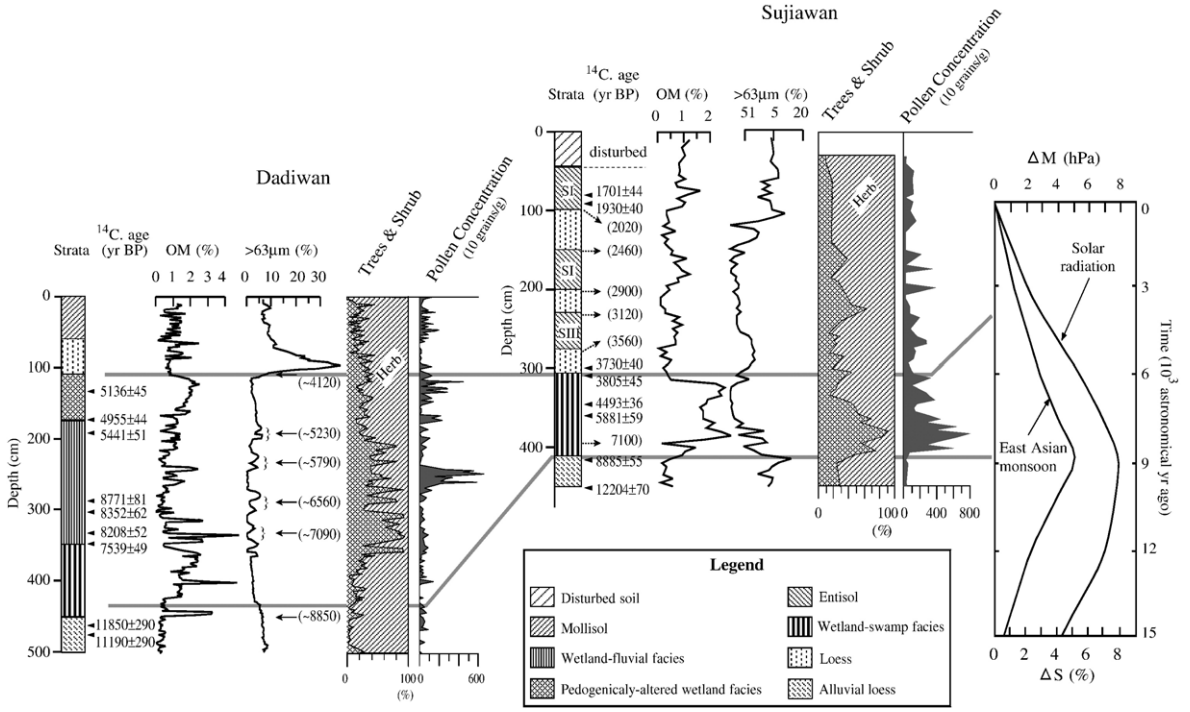

Fig. 9. Comparison between Dadiwan and Sujiawan sections with reference to the insolation trend in the middle latitudes (Δ*S*) and the associated strength of the East Asian Monsoon (Δ*M*).

3.4. Summary

3.4.1. Early–middle Holocene

The data from the Sujiawan section show that after the massive loess deposition of the late glacial, the wetland–swamp facies was formed from 8880 to 3800 ^{14}C years BP. The pollen assemblages indicate the existence of a temperate forest during the early part (8880–4490 ^{14}C years BP) and the existence of a Compositae-dominated steppe during the late part (4490–3800 ^{14}C years BP) with the interval between 7100 and 4490 ^{14}C years BP having the densest and most mesic vegetation of the Holocene (Fig. 9). However, aquatic snails reached their maximum abundance from 7100 to 3800 ^{14}C years BP. Our interpretation is that the optimal ecological condition (7100–4490 ^{14}C years BP) was the delayed response of the vegetation to the climate amelioration that had started around 9000 ^{14}C years BP and that the maximal abundance of aquatic snails (7100–3800 ^{14}C years BP) was the delayed response of snail communities to the development of wetland–swamp environmental condition.

The general trend of the early–middle Holocene environmental changes expressed at the Sujiawan section (100 cm thick) is further detailed by the laterally traceable equivalent (i.e., wetland–swamp–fluvial complex) at the Dadiwan section (335 cm thick) where a higher resolution reconstruction was obtained. Specifically, a forest-steppe dominated from 8850 to 7540 ^{14}C years BP and a *Pinus*-dominated forest occupied the landscape from 7540 to 6560 ^{14}C years BP. The densest and most mesic vegetation (a temperate deciduous forest) with the highest pollen concentration (up to 6500 grains/g) occurred from 6560 to 5790 ^{14}C years BP. The vegetation then deteriorated to a *Pinus*-dominated forest-steppe (5790–4950 ^{14}C years BP), which was followed by an *Ulmus*-dominated forest-steppe (4950–4120 ^{14}C years BP). We want to point out that since the fluvial processes-resulted age reversals are chronostratigraphically local, the contamination by fluvially reworked pollen was probably also chronostratigraphically local, thereby redeeming the validity of the pollen zone divisions and thus the environmental interpretations at the Dadiwan section.

As discussed earlier, the Dadiwan section recorded four flooding events (~7090 ^{14}C years BP, ~6560 ^{14}C years BP, ~5790 ^{14}C years BP, ~5230 ^{14}C years BP) during the entire wetland-flooding coupling period (170–355 cm; 7540–4950 ^{14}C years BP) with a quasi-periodicity of 600±150 years. Each one of them was predated by a depositional interval of aquatic snail-rich wetland facies (see Figs. 8 and 9). Two longest (over 800 years) land-surface stable periods of the Holocene are: from 8850 to 7540 ^{14}C years BP and from 4950 to 4120 ^{14}C years BP. The pedogenically-altered wetland-facies upper layer (115–170 cm; 4950–4120 ^{14}C years BP) was probably formed when the climate was still humid and land surface was rather stable, implying that both eolian and fluvial processes were not very active from 4950 to 4120 ^{14}C years BP.

3.4.2. Late Holocene

The Sujiawan section recorded much more details regarding the late Holocene vegetation variations and the associated environmental changes. As indicated by organic matter content, carbonate concentration, particle size, and aquatic snails shown in Figs. 5 and 6, the wetland–swamp complex ended abruptly at 3800 ^{14}C years BP. The subsequent loess unit (3800–3560 ^{14}C years BP) and the overlying paleosol SIII (3560–3120 ^{14}C years BP) are characterized by steppe pollen assemblages. A desert-steppe dominated the landscape from 3120 to 2900 ^{14}C years BP. After a period of vegetation improvement (steppe) during the time of paleosol SII formation (2900–2460 ^{14}C years BP), a desert-steppe resumed (2460–2020 ^{14}C years BP). A steppe vegetation was re-established around 2020 ^{14}C years BP and seems to have deteriorated again around an inferred age of 1000 ^{14}C years BP (at the depth of 50 cm). The late Holocene loess-paleosol couplets appear to have a quasi-periodicity of 350±100 years. It should be stressed that the organic matter content and field-observed pedostratigraphy well identify these late Holocene paleosols and loess units, but pollen assemblages only show general trends of the late Holocene environmental changes.

4. Discussion on forcing mechanisms

The Holocene climatic trend in the western part of the Chinese Loess Plateau seems to have been modulated by the insolation trend. The insolation started to increase around 15,000 years BP (calendar years) and peaked around 9000 years BP when the obliquity-driven seasonality reached the maximum with the summer insolation being about 8% more than the present (COHMAP Members, 1988; Kutzbach and Gallimore, 1988; Clemens et al., 1996; Koutavas et al., 2002). As a result, tropical Holocene SST increased steadily from ~10,000 to ~6000 years BP (Kiennast et al., 2001). This steady increase in tropical SST might have effectively strengthened the East Asian summer monsoon as the COHMAP project predicted (COHMAP

Members, 1988), resulting in the "megahumid" climate in the western part of the Chinese Loess Plateau (Feng et al., 2004, 2005, 2006). Kremenetski et al. (1998) and McDonald et al. (2000) reported that the post-glacial boreal-forest development in Siberia commenced by 10,000 cal. years BP, advanced southward between 9000 and 7000 cal. years BP and retreated northward between 4000 and 3000 cal. years BP. The forest advancement was attributed to a number of temperature-related factors including heightened summer insolation, ice sheet demise, sea-ice cover reduction, and landward penetration of warm North Atlantic water. The forest retreat was interpreted to have resulted from declining summer insolation and cooling arctic water under a neoglacial regime. The timing consistency between the western part of the Chinese Loess Plateau and Siberia implies that the East Asian monsoon-related precipitation in the western part of the Chinese Loess Plateau has probably been modulated by high northern-latitude temperature. Specifically, high temperatures in high northern latitudes might have weakened the strength of the winter monsoon and thus enhanced the strength of the summer monsoon probably via lengthening of the rainy season, directly contributing to the "megahumid" climate between 10,000 and 4000 years BP in the western part of the Chinese Loess Plateau.

One more point we want to make is about the mid-Holocene Climatic Optimum. All published data indicate that the Climatic Optimum (i.e., warm and wet) occurred approximately between 8000 and 5000 years BP during the Megathermal period that lasted approximately from 9000 to 3000 years BP in arid and semiarid North China (see Shi and Kong, 1992; Shi et al., 1993; Wu et al., 1994; Feng et al., 1993, 2004, 2006, and the references thereafter). The Climatic Optimum occurred between 7100 and 4490 ^{14}C years BP in the western part of the Chinese Loess Plateau, as represented by the densest and most mesic vegetation of the Holocene at the Sujiawan section. The time frame of the Climatic Optimum can be further narrowed down by the higher-resolution data from the Dadiwan section, i.e. the highest pollen concentration (up to 6500 grains/g) and the highest deciduous tree pollen percentage (up to 40%) with a dramatic appearance of *Typha* (up to 30%) and Cyperaceae (up to 30%) between 6560 and 5790 ^{14}C years BP represent a temperate deciduous forest landscape with maximum density and diversity of the entire Holocene period. The Climatic Optimum between 6560 and 5790 ^{14}C years BP is most likely the result of the Holocene peak amplitude of the seasonal cycle of insolation in the Northern Hemisphere at about 6000 years BP., i.e. the peak amplitude at around 6000 years BP increased the sea–land temperature contrast, thus further enhancing the East Asian summer monsoon (Kutzbach and Liu, 1997; Brostrom et al., 1998). This scenario is directly supported by the maximum lake levels occurring in India during the increased summer insolation period at around 6000 years BP (Enzel et al., 1999). Indirect evidence supportive for this scenario is the maximum Holocene aridity in South America (Baker et al., 2001) and the weakening Australian monsoon during the decreased summer insolation period in the Southern Hemisphere at around 6000 years BP (Steig, 1999; Koutavas et al., 2002).

Acknowledgement

This research is financially supported by three NSFC Grants (No. 40331012, No. 40025105, and No. 404321101), and also by two NSF grants (EAR 0402509 and BCS 00-78557). Two anonymous reviewers are sincerely thanked for their constructive comments.

References

An, C.B., 2004. Holocene Environmental Changes in the Western Part of the Chinese Loess Plateau and its Effects on Prehistoric Cultural Development. Ph.D. Dissertation of Lanzhou University (in Chinese).

An, Z.S., Kukla, G., Porter, S.C., Xiao, J., 1991. Magnetic susceptibility evidence of monsoon variation on the Loess Plateau of central China during the last 130000 years. Quat. Res. 36, 29–36.

An, Z.S., Porter, S.C., Wu, X.H., 1993. Holocene Climatic Optimum and associated East Asian Monsoon in eastern China. Chin. Sci. Bull. 38 (14), 1302–1305 (in Chinese).

An, Z.S., Porter, S.C., Kutzbach, J.E., Wu, X., Wang, S., Liu, X., Li, X., Zhou, W., 2000. Asynchronous Holocene optimum of the East Asia monsoon. Quat. Sci. Rev. 19, 743–762.

Baker, P.A., Seltzer, G.O., Fritz, S.C., Dunbar, R.B., Grove, M.J., Tapia, P.M., Cross, S.L., Rowe, H.D., Broda, J.P., 2001. The history of South American tropical precipitation for the past 25,000 years. Science 291, 640–643.

Brostrom, A., Coe, M., Harrison, S.P., Gallimore, R., Kutzbach, J.E., Foley, J., Prentice, I.C., Behling, P., 1998. Land surface feedbacks and paleomonsoon in North Africa. Geophys. Res. Lett. 25 (19), 1618–3615.

Chen, F.H., Boemendal, J., Feng, Z.-D., Wang, J.-M., Zhou, Z.-T., Park, E., Shi, Y., 1999. Last Interglacial East Asian monsoon variation: evidence from the western part of Chinese Loess Plateau. Quat. Sci. Rev. 18, 1127–1135.

Chen, F.H., Feng, Z.-D., Zhang, J.W., 2000. Loess particle size data indicative of stable winter monsoon during the last interglacial in the western part of Chinese Loess Plateau. Catena 39, 233–244.

Clemens, S.C., Murray, D.W., Prell, W.L., 1996. Nonstationary phase of the Plio-Pleistocene Asian Monsoon. Science 274, 943–948.

COHMAP Members, 1988. Climatic changes of the last 18,000 years: observation and modeling. Science 241, 1043–1052.

Enzel, Y., Ely, L.L., Mishra, S., Ramesh, R., Amit, R., Lazar, B., Rajaguru, S.N., Baker, V.R., Sandler, A., 1999. High-resolution

Holocene environmental changes in the Thar Desert, northwestern India. Science 284, 125–128.
Feng, Z.-D., Thompson, L.G., Mosley-Thompson, E., Yao, T.D., 1993. Temporal and spatial variations of climate in China during the last 10,000 years. Holocene 3 (2), 174–180.
Feng, Z.-D., An, C.B., Tang, L.Y., Jull, A.J.T., 2004. Stratigraphic evidence of megahumid mid-Holocene climate in the western part of the Chinese Loess Plateau. Glob. Planet. Change 43, 145–155.
Feng, Z.-D., Wang, W.G., Guo, L.L., Li, X.Q., Ma, Y.Z., Zhang, H.C., An, C.B., 2005. Holocene climate changes in the Mongolian Plateau: preliminary results. Quat. Int. 136, 25–32.
Feng, Z.-D., An, C.B., Wang, H.B., 2006. Holocene climatic and environmental changes in the arid and semiarid regions of China: a review. Holocene 16, 119–130.
Gao, S.Y., Chen, W.N., Jin, H.L., Dong, G.R., Li, B.S., Yang, G.S., Liu, L.Y., Guan, Y.Z., Sun, Z., Jin, J., 1993. East Asian Monsoon variations in the desert areas of the Inner Mongolia during the Holocene. Sci. China (B) 23 (2), 202–208 (in Chinese).
Kiennast, M., Steinke, S., Stattegger, K., Calvert, S.E., 2001. Synchronous tropical South China Sea SST change and Greenland warming during deglaciation. Science 291, 2131–3134.
Kremenetski, C.V., Sulerzhitsky, I.D., Hantemirov, R., 1998. Holocene history of the northern rang limits of some trees and shrubs in Russia. Arct. Alp. Res. 30 (4), 317–333.
Koutavas, A., Lynch-Stieglitz, J., Marchitto, T.W., Sachs, J.P., 2002. El Nino-like pattern in ice age Tropical Pacific sea surface temperature. Science 297, 226–229.
Kutzbach, J., Gallimore, R.G., 1988. Sensitivity of a coupled atmosphere and mixed-layer ocean model to changes in orbital forcing at 9000 yr B.P. J. Geophys. Res. 93, 803–821.
Kutzbach, J.E., Liu, Z., 1997. Response of the African monsoon at orbital forcing and ocean feedbacks in the middle Holocene. Science 278, 440–443.
Li, W.Y., 1998. Quaternary Vegetation Variations and the Associated Environmental Changes in China. Science Press, Beijing (in Chinese).
Li, J.J., Feng, Z.-D., Tang, L.Y., 1988. Late Quaternary monsoonal patterns in the Loess Plateau of China. Earth Surf. Processes Landf. 13, 125–135.
Liu, T.S., 1987. Loess and Environments. Ocean Press, Beijing.
Liu, H.Y., Cui, H.T., Pott, R., 1999. The surface pollen of the woodland-steppe ecotone in southeastern Inner Mongolia. Rev. Palaeobot. Palynol. 105, 237–250.
Ma, Y.Z., 2004. Late Cenozoic vegetation history and associated environmental changes in Northeastern margin of the Tibet Plateau. Ph.D. Dissertation, Lanzhou University (in Chinese).
Ma, Y.Z., Zhang, H.C., Pachur, H.J., Wunnemann, B., Li, J.J., Feng, Z.-D., 2004. Modern pollen-inferred Holocene climate change in the Tengger Desert, NW China. Holocene 14 (6), 841–850.
McDonald, G.M., Velichko, A.A., Kremenetski, C.V., Borisova, O.K., Goleva, A.A., Andreev, A.A., Cwynar, L.C., Riding, R.T., Forman, S.L., Edwards, T.W.D., Aravena, R., Hammarlund, D., Szeicz, J. M., Gattaulin, V.N., 2000. Holocene treeline history and climate change across Northern Eurasia. Quat. Res. 53, 302–311.
Maher, B.A., 1998. Magnetic properties of modern soils and Quaternary loessic palaeosols: paleoclimatic implications. Palaeogeogr. Palaeoclimatol. Palaeoecol. 137, 25–54.
Moore, P.H., Webb, J.A., Collinson, M.E., 1991. Pollen Analysis, 2nd ed. Blackwell Scientific Publications, London.
Shi, Y.F., Kong, Z.C., 1992. The Holocene Climatic Optimum and Associated Environment in China. Science Press, Beijing (in Chinese).
Shi, Y.F., Kong, Z.C., Wang, S.M., Tang, L.Y., Wnag, F.B., Yao, T.D., Zhao, X.T., Zhang, P.Y., Shi, S.H., 1993. The mid-Holocene megathermal climate and environment in China. Sci. China, Ser B 23 (8), 865–873 (in Chinese).
Singer, M., Janitzky, P., 1987. Field and Laboratory Procedures Used in Soil Chronosequence Study. U.S.G.S. Bulletin, 1648.
Steig, E.J., 1999. Mid-Holocene climate change. Science 286, 1485–1487.
Stuiver, M., Reimer, P.J., Bard, E., Beck, J.W., Burr, G.S., Hughen, K. A., Kromer, B., McCormac, F.G., Plicht, J., Spurk, M., 1998. Calib 4. Radiocarbon 40, 1041–1083.
Tang, L.Y., Feng, Z.-D., Kang, J.C., 1990. Pollen assemblages and their depositional environments in the boundary area between the Tibet and Loess Plateaus of China. J. Glaciol. Geocryol. 12, 125–139 (in Chinese).
Tong, G.B., Yang, Z.D., Wang, S.M., Xia, L.H., 1996. Surface pollen spectrum and its characteristics along a transect from Madira to Dayangshu in NE China. Acta Bot. Sin. 38, 814–821 (in Chinese).
Wang, H.B., 2001. Climate changes during the last three interglacials documented by high-resolution loess sequences. Masters Thesis of Lanzhou University (in Chinese).
Wang, S.L., Xu, Q.Z., 1988. Vegetation variations since the late Pleistocene in Saleshan Mountain area, Gansu Province of China. In: Zeng, S.W., et al. (Ed.), Symposium of Landslides in China. Railroad Press, pp. 230–232 (in Chinese).
Wang, F.X., Qian, N.F., Zhang, Y.L., Yang, H.Q., 1995. Pollen Flora of China. Science Press, Beijing (in Chinese).
Wang, B.Y., Song, C.Q., Sun, X.J., 1996. Surface pollen assemblages in the Inner Mongolian Plateau. Acta Bot. Sin. 38 (11), 902–909 (in Chinese).
Wu, G.H., Jiang, C.Y., 1998. Natural Geographic Characteristics of Gansu Province. Gansu Science and Technology Press, Lanzhou (in Chinese).
Wu, X.H., An, Z.S., Wang, S.M., 1994. Temporal and spatial variations in the East Asian Monsoon during the Holocene. Quat. Sci. 1, 24–35 (in Chinese).
Xu, Q.H., Yang, X.L., Liang, W.D., 2000. Study of pollen dispersing processes in Yanshan area of Hebei Province of China. Geogr. Land Resour. 16, 54–62 (in Chinese).
Yan, S., Xu, Y.Q., 1989. Surface pollen assemblages in Xinjiang of China. J. Arid Land Res. 1, 26–33 (in Chinese).
Zhao, J.B., Yue, Y.L., Yue, M., 1998. Pollen assemblages of *Quercus* forests in the Qinling Mountains and in the Chinese Loess Plateau. J. Xi'an Inst. Eng. Technol. 20 (1), 46–50 (in Chinese).
Zhao, C.Y., Nan, Z.R., Feng, Z.-D., 2004. GIS-assisted modeling of the potential eco-hydrologic conditions in the western part of the Chinese Loess Plateau. J. Arid Environ. 58, 387–403.
Zhou, S.Z., Chen, F.H., Pan, B.T., Cao, J.X., Li, J.J., Derbyshire, E., 1991. Environmental change during the Holocene in western China on a millennial timescale. The Holocene 1/2, 151–156.
Zhou, W.J., Donahue, D.J., Porter, S.C., Jull, T.A., Li, X.Q., Stuiver, M., An, Z.S., Matsumoto, E., Dong, G.R., 1996. Variability of monsoon climate in East Asia at the end of the last glaciation. Quat. Res. 46, 219–229.
Zhou, W.J., Head, M.L., Lu, X.F., 1999. Teleconnection of climatic events between East Asia and polar high latitude areas during the last deglaciation. Palaeogeogr. Palaeoclimatol. Palaeoecol. 152, 163–172.